Vibronic Interactions and Possible Electron Pairing in the Photoinduced Excited Electronic States in Molecular Systems: A Theoretical Study

Takashi Kato* and Tokio Yamabe

Institute for Innovative Science and Technology, Graduate School of Engineering, Nagasaki Institute of Applied Science, 3-1, Shuku-machi, Nagasaki 851-0121, Japan

Received: September 30, 2004; In Final Form: February 25, 2005

Electron−phonon interactions in the photoinduced excited electronic states in molecular systems such as phenanthrene-edge-type hydrocarbons are discussed and compared with those in the monoanions and cations. The complete phase patterns difference between the highest occupied molecular orbitals (HOMO) and the lowest unoccupied molecular orbitals (LUMO) (the atomic orbitals between two neighboring carbon atoms combined in phase (out of phase) in the HOMO are combined out of phase (in phase) in the LUMO) are the main reason that the C−C stretching modes around 1500 cm^{-1} afford much larger electron−phonon coupling constants in the excited electronic states than in the charged electronic states. The frequencies of the vibrational modes that play an essential role in the electron−phonon interactions for the excited electronic states are similar to those for the monoanions and cations in phenanthrene-edge-type hydrocarbons. Possible electron pairing and Bose−Einstein condensation in the photoinduced excited electronic states as well as those in the monoanions and cations in molecular systems such as phenanthrene-edge-type hydrocarbons are also discussed.

Introduction

In modern physics and chemistry, the effect of vibronic interactions[1] in molecules and crystals has been an important topic. The analysis of vibronic interaction theory covers a large variety of research fields such as spectroscopy, instability of molecular structure, electrical conductivity,[2] and superconductivity. Electron−phonon coupling[1,2,4] is the consensus mechanism for attractive electron−electron interactions in the Bardeen−Cooper−Schrieffer (BCS) theory of superconductivity.[5,6] Since Little's proposal for a possible molecular superconductor based on an exciton mechanism,[7] the superconductivity of molecular systems has been extensively investigated. Although such a unique mechanism has not yet been established, advances in the design and synthesis of molecular systems have yielded a lot of BEDT-TTF-type organic superconductors,[8] where BEDT-TTF is bis(ethylenedithio)tetrathiafulvalene. An inverse isotope effect due to substituting hydrogen by deuterium in organic superconductivity was observed by Saito et al.[9] The alkali-metal-doped A_3C_{60} complexes[10] were found to exhibit superconducting transition temperatures (T_cs) of more than 30 K (ref 11) and 40 K under pressure.[12] In alkali-metal-doped fullerenes,[13] pure intramolecular Raman-active modes have been suggested to be important in a BCS-type[5] strong-coupling scenario in superconductivity.

In previous work, we have analyzed the vibronic interactions and estimated possible T_cs in the monocations of acenes based on the hypothesis that the vibronic interactions between the intramolecular vibrations and the highest occupied molecular orbitals (HOMO) play an essential role in the occurrence of superconductivity in positively charged nanosized molecular systems.[14] On the basis of an experimental study of ionization spectra using high-resolution gas-phase photoelectron spectroscopy, electron−phonon interactions in positively charged acenes were studied recently.[15] The experimental results showed that our predicted frequencies for the vibrational modes, which play an essential role in the electron−phonon interactions,[14] as well as the predicted total electron−phonon coupling constants[14] are in excellent agreement with those obtained from experimental research.[15]

Polyacenic semiconductor (PAS) materials, which are prepared from phenol-formaldehyde resin at relatively low temperatures,[16a,b] belong to a typical amorphous carbon (a-C) material. From structural analyses of PAS and polynuclear aromatic hydrocarbons (PAH) materials,[16] it has been demonstrated that they have content similar to that of aromatic carbons but a different graphite sheet shape, that is, different edge structures.[16c] Numerous 1-D PAHs have been theoretically and numerically investigated by several researchers.[17−23] Their sizes and especially their edge structures are closely related to the electronic properties of PAHs.[20−28] According to their edge structures, PAHs can usually be classified into two main groups: acene-edge-type and phenanthrene-edge-type. The two structures show remarkably different electronic features. The superconductivity of phenanthrene-edge-type hydrocarbons has not yet been found until now, but it is of interest to investigate the vibronic interactions and the possible electron−electron pairing in various electronic states in this molecular system.

We have studied the condition under which the charged nanosized molecules exhibit strong electron−phonon interactions and have found that the electron−phonon interactions in charged molecular systems become weaker with an increase in molecular size.[14c] From our calculated results, we can expect the electron−phonon interactions to become stronger with an increase in the number of carriers per atom. The purpose of this paper is to investigate the electron−phonon interactions in

* To whom correspondence should be addressed. E-mail: kato@cc.nias.ac.jp. Phone: +81-95-838-4363. Fax: +81-95-838-5105.

10.1021/jp040643r CCC: $30.25
Published on Web 05/11/2005

SCHEME 1

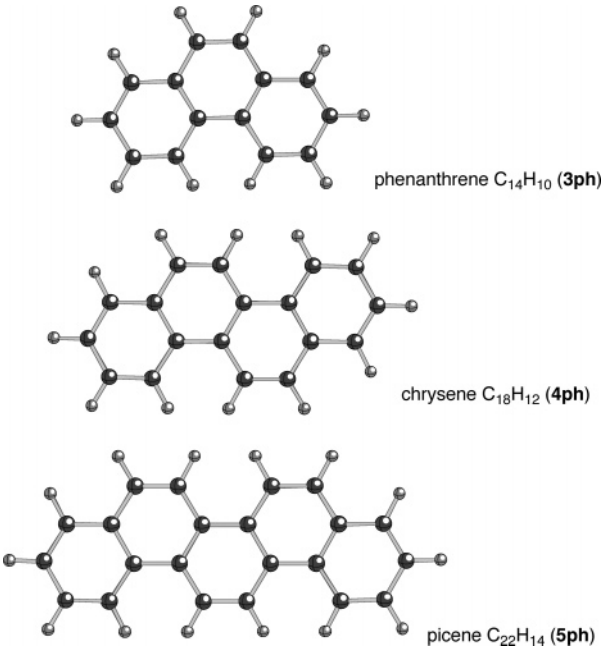

the photoinduced excited electronic states of molecular systems and to compare the calculated results with those for the negatively and positively charged molecular systems.[29] As an example, we will consider phenanthrene-edge-type hydrocarbons (phenanthrene $C_{14}H_{10}$ (**3ph**), chrysene $C_{18}H_{12}$ (**4ph**), and picene $C_{22}H_{14}$ (**5ph**) (Scheme 1)) in this study. We will suggest a reason for the total electron−phonon coupling constants for the excited electronic states being much larger than those for the negatively and positively charged molecular systems in view of the orbital patterns of the frontier orbitals in detail. We have investigated the electron−phonon interactions in the monoanions and cations of molecular systems.[14] That is, we have considered the monoanions and cations in which electrons partially occupying the conduction band and partially occupying the valence band, formed by the lowest unoccupied molecular orbitals (LUMO) and the HOMO, respectively, of each molecule, play an essential role in the electrical conductivity (Figure 1a and b). We will also consider photoinduction instead of charge doping in this study. That is, we consider the electron−phonon interactions in the photoinduced excited electronic states in this study, in which electrons partially occupying the valence band as well as partially occupying the conduction band formed by the HOMO and LUMO of each molecule, respectively, play an essential role in the electron−phonon interactions and in electrical conductivity (Figure 1c). We also discuss the possible electron pairing and Bose−Einstein condensation in these electronic states. Even though we consider only phenanthrene-edge-type hydrocarbons in this study as an example, our method in this study is applicable to studies of various nanosized molecules.

Theoretical Background

Let us first consider the basic optical features of **3ph**. We will use small letters for one-electron orbital symmetries and capital letters for the symmetries of both electronic and vibrational states, as usual. The symmetry labels of the HOMO and the LUMO of **3ph** are b_1 and a_2, respectively. According to the character table for the C_{2v} point group, the $A_1 \rightarrow B_2$ transition is optically allowed. Thus, from the direct product of the orbital symmetries in eq 1, such an allowed $A_1 \rightarrow B_2$ optical

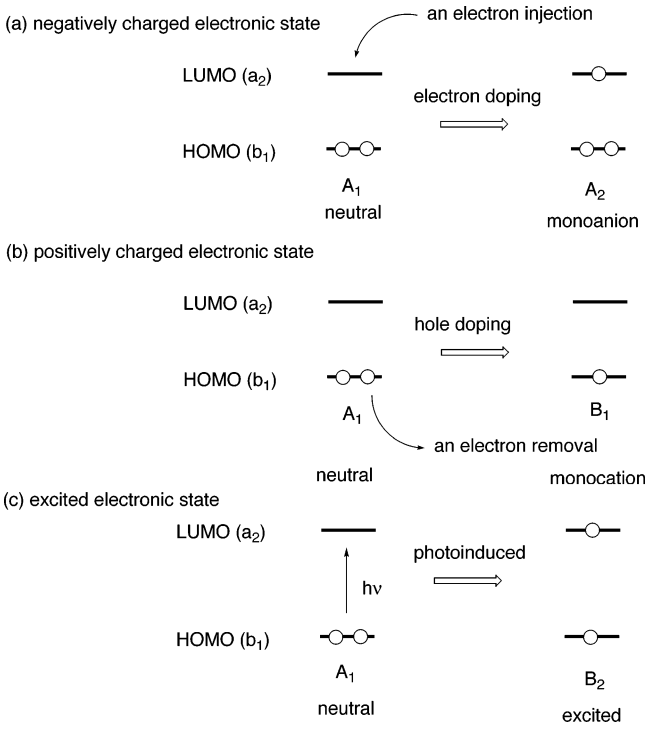

Figure 1. Frontier orbitals and possible lowest optically allowed transitions in phenanthrene-edge-type hydrocarbons.

absorption occurs when an electron in the b_1 HOMO is promoted to the a_2 LUMO in **3ph**, as shown in Figure 1c.

$$b_1 \times a_2 = B_2 \tag{1}$$

Vibronic Interactions between the Nondegenerate Frontier Orbitals and the Totally Symmetric Vibrational Modes in Phenanthrene-Edge-Type Hydrocarbons. We discuss the theoretical background for the orbital vibronic interactions in phenanthrene-edge-type hydrocarbons. The potential energy for the neutral ground state, negatively and positively charged electronic states, and the excited electronic state in **3ph** is shown in Figure 2. Here, we take a one-electron approximation into account; the vibronic coupling constants of the vibrational modes to the electronic states in the monoanions and cations and to the excited B_2 electronic states of **3ph** are defined as the sum of orbital vibronic coupling constants from all of the occupied orbitals,[3a]

$$g_{\text{electronic state}} = \sum_{i}^{\text{occupied}} g_i \tag{2}$$

Considering the one-electron approximation and that the first derivatives of the total energy vanish in the ground state for the equilibrium structure in neutral phenanthrene-edge-type hydrocarbons (i.e., $g_{\text{neutral}} = \sum_i^{\text{HOMO}} g_i = 0$) (Figure 2a) and that one electron must be injected into (removed from) the LUMO (HOMO) to generate the monoanions (monocations), the vibronic coupling constants of the totally symmetric vibrational modes to the electronic states of the monoanions and cations of phenanthrene-edge-type hydrocarbons can be defined by eqs 3 and 4, respectively,

$$g_{\text{monoanion}}(\omega_m) = g_{\text{LUMO}}(\omega_m) \tag{3}$$

$$g_{\text{monocation}}(\omega_m) = g_{\text{HOMO}}(\omega_m) \tag{4}$$

In this paper, we focus upon the diagonal processes; only the

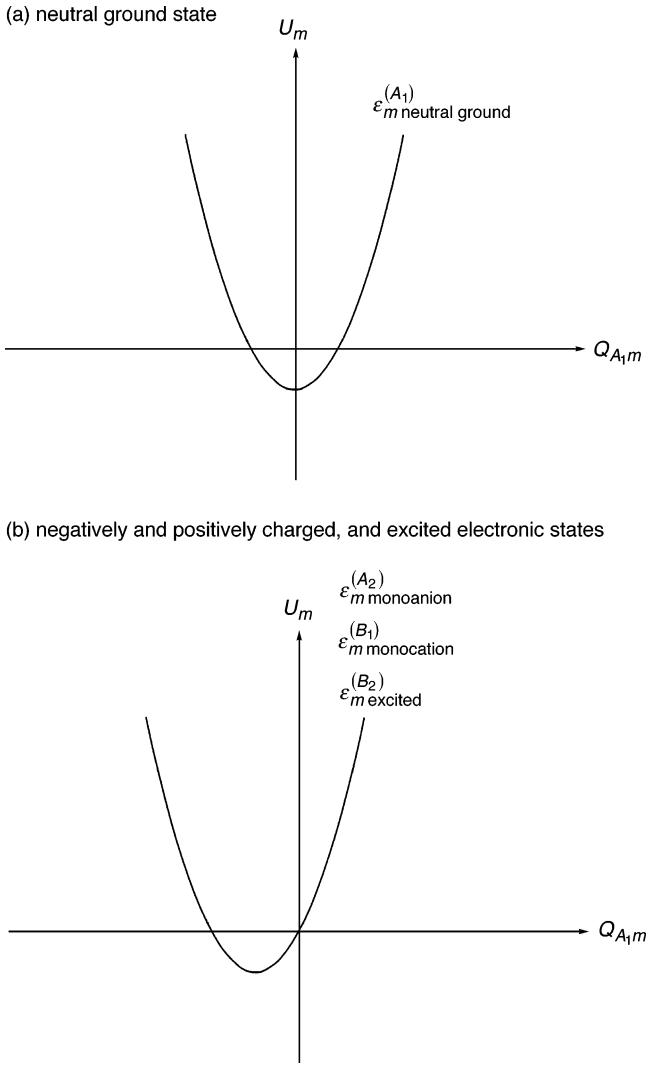

Figure 2. Energy levels of (a) the ground states and (b) the negatively, positively, and excited electronic states as a function of the normal coordinate for A_1 symmetry.

electronic states that belong to the same irreducible representations are considered. Thus, the symmetry of the vibronic active modes can be defined from the direct product of the orbital symmetries as follows:

$$b_1 \times b_1 = a_2 \times a_2 = A_1 \tag{5}$$

Therefore, the totally symmetric A_1 vibrational modes couple to the b_1 HOMO and a_2 LUMO in **3ph**. The number of totally symmetric modes is 23, 29, and 35 for **3ph**, **4ph**, and **5ph**, respectively. In such a case, we must consider multimode problems, but in the limit of linear vibronic coupling, one can treat each set of modes (i.e., each mode index m) independently.[3]

Let us look into the vibronic interaction between the A_1 modes and the HOMO and LUMO. The dimensionless orbital vibronic coupling constants of the totally symmetric modes in phenanthrene-edge-type hydrocarbons are defined by

$$g_{\mathrm{HOMO}}(\omega_m) = \frac{1}{\hbar\omega_m}\left\langle \mathrm{HOMO}\middle|\left(\frac{\partial h}{\partial q_{\mathrm{A}_1 m}}\right)_0\middle|\mathrm{HOMO}\right\rangle \tag{6}$$

$$g_{\mathrm{LUMO}}(\omega_m) = \frac{1}{\hbar\omega_m}\left\langle \mathrm{LUMO}\middle|\left(\frac{\partial h}{\partial q_{\mathrm{A}_1 m}}\right)_0\middle|\mathrm{LUMO}\right\rangle \tag{7}$$

where q_{A_1m} is the dimensionless normal coordinate[30] of the mth vibrational mode and is expressed by using the normal coordinate Q_{A_1m} as

$$q_{\mathrm{A}_1 m} = \sqrt{\frac{\omega_m}{\hbar}} Q_{\mathrm{A}_1 m} \tag{8}$$

Vibronic Interactions between the Excited B_2 Electronic States and the A_1 Vibrational Modes in Phenanthrene. We next discuss the vibronic interactions between the excited B_2 electronic states and the vibrational frequency modes in **3ph**. As mentioned earlier, the lowest optically allowed transition occurs when an electron in the HOMO is promoted to the LUMO. Changes in the HOMO and LUMO levels in phenanthrene-edge-type hydrocarbons by displacements of the totally symmetric A_1 vibrational modes are shown in Figure 3. Let us consider the one-electron promotion from the HOMO to the LUMO in **3ph**. For example, when **3ph** is distorted along the A_1 mode of 1434 cm^{-1}, the HOMO and LUMO are destabilized and stabilized in energy, respectively, as shown in Figure 3d-i. However, when it is distorted along the A_1 mode of 266 cm^{-1}, both the HOMO and LUMO are stabilized, as shown in Figure 3d-ii. Considering the one-electron approximation[3] mentioned above and the fact that the first derivatives of the total energy vanish in the ground state for the equilibrium structure (Figure 2 (a)), we can define the vibronic coupling constants of the excited B_2 electronic state to the A_1 vibrational mode in the case of Figure 3d-i in phenanthrene-edge-type hydrocarbons by[31]

$$g_{\mathrm{B}_2(\mathrm{HOMO}\rightarrow\mathrm{LUMO})}(\omega_m) = \frac{1}{\hbar\omega_m}\left\langle \mathrm{B}_2\middle|\left(\frac{\partial h}{\partial q_{\mathrm{A}_1 m}}\right)_0\middle|\mathrm{B}_2\right\rangle = |g_{\mathrm{HOMO}}(\omega_m)| + |g_{\mathrm{LUMO}}(\omega_m)| \tag{9}$$

and those in case of Figure 3d-ii in phenanthrene-edge-type hydrocarbons by

$$g_{\mathrm{B}_2(\mathrm{HOMO}\rightarrow\mathrm{LUMO})}(\omega_m) = \frac{1}{\hbar\omega_m}\left\langle \mathrm{B}_2\middle|\left(\frac{\partial h}{\partial q_{\mathrm{A}_1 m}}\right)_0\middle|\mathrm{B}_2\right\rangle = ||g_{\mathrm{HOMO}}(\omega_m)| - |g_{\mathrm{LUMO}}(\omega_m)|| \tag{10}$$

Electron−Electron Interactions Mediated by the Emission and Absorption of a Virtual Phonon. In the BCS theory of superconductivity,[5] we consider the electron−electron interaction arising from the exchange of a virtual phonon as a scattering process. There are two intermediate states allowed by momentum conservation. An electron with wave vector $\mathbf{k}$ emits a phonon of wave vector $-\mathbf{q}$ to scatter it into $\mathbf{k} + \mathbf{q}$. This phonon is then absorbed by another electron with $-\mathbf{k}$ to scatter it into a state $-\mathbf{k} - \mathbf{q}$. Such a short-lived phonon is called the virtual phonon, and the scattering involved is called the virtual phonon process. We combine this electron−electron interaction arising from the electron−phonon coupling with the Coulomb repulsive interactions between the electrons.[32] To consider the electron pairing in molecular systems, we write the electron−electron interaction $V_{\mathbf{k}+\mathbf{q},\mathbf{k}}$ in the form of the BCS reduced Hamiltonian[5,32] shown below

$$V_{\mathbf{k}+\mathbf{q},\mathbf{k}} = \frac{V_{\mathbf{q}}^* V_{\mathbf{q}} \hbar\omega_{\mathbf{q}}}{(\epsilon_{\mathbf{k}} - \epsilon_{\mathbf{k}+\mathbf{q}})^2 - (\hbar\omega_{\mathbf{q}})^2} + V_{\mathbf{k}+\mathbf{q},\mathbf{k}}^{\mathrm{Coulomb}} \tag{11}$$

where $V_{\mathbf{k}+\mathbf{q},\mathbf{k}}^{\mathrm{Coulomb}}$ denotes the Coulomb interaction among electrons, which is always positive (repulsive). To achieve an overall

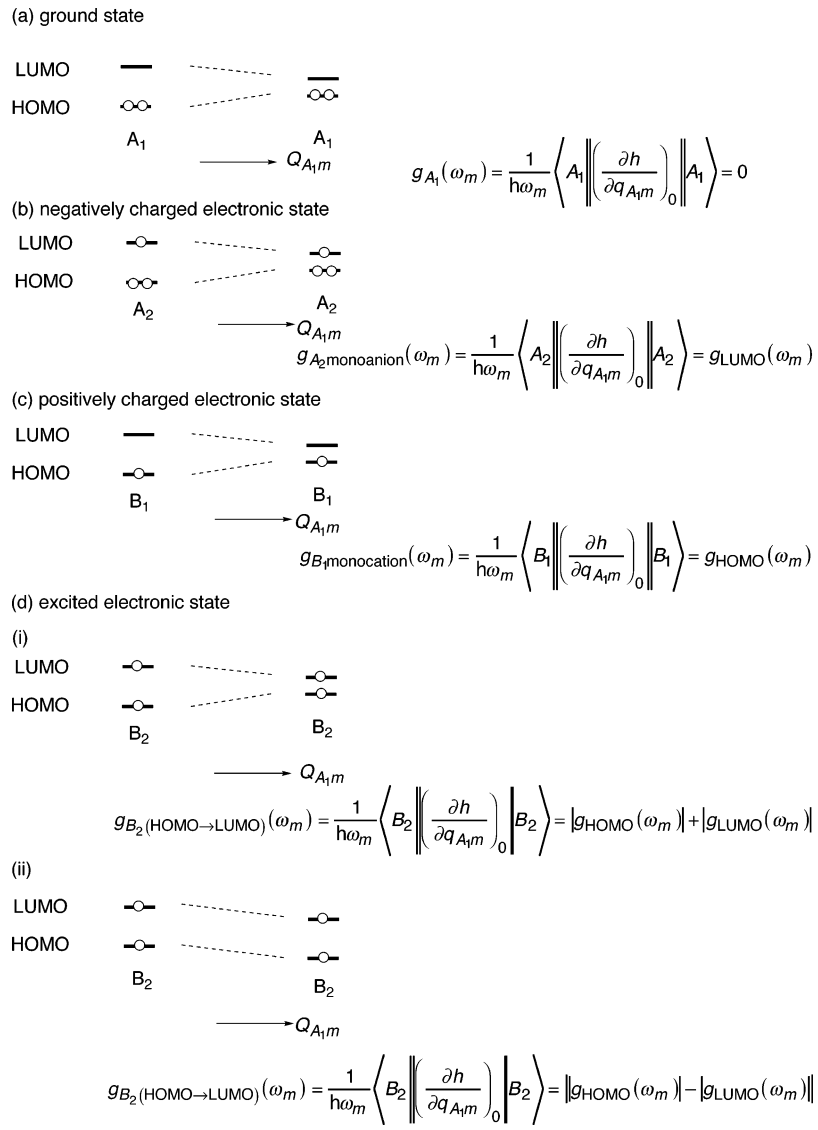

Figure 3. Changes of the HOMO and the LUMO levels in phenanthrene-edge-type hydrocarbons by displacements of the totally symmetric vibrational modes.

attractive interaction between electrons (electronic states), we have

$$V_{\mathbf{k}+\mathbf{q},\mathbf{k}} = \frac{V_{\mathbf{q}}^* V_{\mathbf{q}} \hbar\omega_{\mathbf{q}}}{(\epsilon_{\mathbf{k}} - \epsilon_{\mathbf{k}+\mathbf{q}})^2 - (\hbar\omega_{\mathbf{q}})^2} + V_{\mathbf{k}+\mathbf{q},\mathbf{k}}^{\text{Coulomb}} < 0 \quad (12)$$

If $|\epsilon_{\mathbf{k}} - \epsilon_{\mathbf{k}+\mathbf{q}}| < \hbar\omega_{\mathbf{q}}$, the first term of eq 12 becomes negative. This process would give rise to a weak but attractive interaction between the two electrons and is taken as a possible mechanism to stabilize the superconducting state.

The mobility of an electron is described by the coupling between a conducting electron and molecular vibrations as the time-dependent phenomenon between $|i\rangle$ and $|j\rangle$. However, following BCS theory, if we consider a two-electron interaction (retarded) induced by phonon ω_m, it gives the well-known terms as the second-order matrix element coupling two electronic states ψ_i and ψ_j even in a molecular system,

$$V_{\text{int}}^{(i,j)} = \sum_m \frac{|\left\langle \psi_i \left| \left(\frac{\partial V}{\partial Q_m}\right)_0 \Delta Q_m \right| \psi_j \right\rangle|^2 \hbar\omega_m}{(\epsilon_i - \epsilon_j)^2 - (\hbar\omega_m)^2} + V_{i,j}^{\text{Coulomb}} \quad (13)$$

$$V_{i,j}^{\text{Coulomb}} \propto \frac{1}{|\boldsymbol{r}_i - \boldsymbol{r}_j| + (\text{const})} \quad (14)$$

The (const) is a consequence of shielding. As a matter of course, such an interaction energy contributes to the Cooper-pair attractive energy in BCS theory for $\epsilon_i \approx \epsilon_j$. After the conventional Fröhlich transformation,[33] $V_{\text{int}}^{(i,j)}$ is expressed by eq 11. In this research, we do not treat the higher-order couplings beyond first order or the electron−phonon interactions originating from intermolecular orbital interactions, as discussed later, which are usually much weaker than the first-order electron−phonon interactions originating from intramolecular orbital interactions in small molecules. In conventional superconductivity in solids, the energy-level differences between crystal orbitals (bands) are very small, thus the higher-order couplings would often be essential. However, in molecular systems, the energy differences between molecular orbitals, for example, the HOMO and LUMO of each molecule, which form valence and conduction bands, respectively, are much larger. In such cases, the first-order coupling constant is much larger than the higher-order coupling constants. Of course, for cases in which the energy difference between two electronic states is very small, the higher-order couplings originating from the interactions between them would

be somewhat important; however, compared with those in the conventional superconductivity, such a higher-order effect would be much less important in small molecules. For a two-level model in the photoinduced excited electronic states, in addition to the diagonal couplings to the totally symmetric phonons, there is the pseudo-Jahn−Teller coupling to the phonons mixing the two levels, which is not treated in this study. For example, in **3ph**, the lowest optically allowed transition occurs when an electron in the b_1 HOMO is promoted to the a_2 LUMO, and the second lowest optically allowed transition occurs when an electron in the b_1 HOMO is promoted to the a_2 LUMO + 3. Therefore, the pseudo-Jahn−Teller coupling originating from the interactions between such two electronic states expressed by the first term of eq 15 as well as the first-order vibronic interactions treated in this study would somewhat play a role in the attractive electron−electron interactions.

$$V_{\mathrm{int}}^{(B_2(\mathrm{HOMO}\rightarrow\mathrm{LUMO}),B_2(\mathrm{HOMO}\rightarrow\mathrm{LUMO}+3))} = \sum_m \frac{|\left\langle \psi_{B_2(\mathrm{HOMO}\rightarrow\mathrm{LUMO})} \left| \left(\frac{\partial V}{\partial Q_m}\right)_0 \Delta Q_m \right| \psi_{B_2(\mathrm{HOMO}\rightarrow\mathrm{LUMO}+3)} \right\rangle|^2 \hbar\omega_m}{(\epsilon_{B_2(\mathrm{HOMO}\rightarrow\mathrm{LUMO})} - \epsilon_{B_2(\mathrm{HOMO}\rightarrow\mathrm{LUMO}+3)})^2 - (\hbar\omega_m)^2} + V_{B_2(\mathrm{HOMO}\rightarrow\mathrm{LUMO}),B_2(\mathrm{HOMO}\rightarrow\mathrm{LUMO}+3)}^{\mathrm{Coulomb}} \quad (15)$$

In particular, the energy difference between two electronic states (or molecular orbitals) becomes smaller with an increase in molecular size. In this case, such pseudo-Jahn−Teller coupling can play an essential role in the attractive electron−electron interactions as in the case of the conventional superconductivity in solids. However, in this study, we consider the first-order electron−phonon coupling in the photoinduced excited electronic states in small molecules with large energy differences between molecular orbitals to compare these results with those in the charged electronic states studied in previous research.[29]

Electron−Phonon Coupling Constants for the Excited Electronic States of Phenanthrene-Edge-Type Hydrocarbons. Let us next discuss the total electron−phonon coupling constants (l_{total}) in the excited electronic states. Because l_{total} is the sum of the electron−phonon coupling constants originating from both intramolecular vibrations (l_{intra}) and intermolecular vibrations (l_{inter}), l_{total} is defined as

$$l_{\mathrm{total}} = l_{\mathrm{intra}} + l_{\mathrm{inter}} \quad (16)$$

However, it should be noted that the intramolecular orbital interactions are much stronger than the intermolecular orbital interactions. Therefore, it is rational that the l_{intra} values are much larger than the l_{inter} values in molecular systems. In fact, it is considered by several researchers that the contribution from the intramolecular modes in molecular systems is decisive in the pairing process in the superconductivity in doped C_{60}.[13,34] For example, it was reported that the l_{intra} values are much larger than the l_{inter} values in K_3C_{60} and Rb_3C_{60} ($l_{\mathrm{intra}} \geq 10 l_{\mathrm{inter}}$).[34] Furthermore, it has also been shown from a neutron-scattering investigation[35] that the electron-libration intramolecular-mode coupling is small in alkali-metal-doped C_{60}. Therefore, we consider only intramolecular electron−phonon coupling in this study. The l_{total} value for the charged and excited electronic states can be defined as

$$l_{\mathrm{total}} \approx l_{\mathrm{intra}} = l_{\mathrm{LUMO}} \quad \text{(for the electronic state of the monoanion)} \quad (17)$$

$$= l_{\mathrm{HOMO}} \quad \text{(for the electronic state of the monocation)} \quad (18)$$

$$= l_{B_2(\mathrm{HOMO}\rightarrow\mathrm{LUMO})} \quad \text{(for the excited electronic state)} \quad (19)$$

In the previous section, the vibronic interactions in free phenanthrene-edge-type hydrocarbons were discussed. We can derive l_{total} by using the vibronic coupling constants defined in eqs 6, 7, 9, and 10 as follows. As described above, because phenanthrene-edge-type hydrocarbons would consist of strongly bonded molecules arranged on a lattice with weak van der Waals intermolecular bonds, we can derive the dimensionless electron−phonon coupling constant λ_m in a similar way as in theory in previous research.[14,29] We use a standard expression for λ_m,[13,14,29]

$$\lambda_m = \frac{2}{N(0)} \sum_{\mathbf{q}} \sum_{\mathbf{k},\mathbf{k}'} \frac{1}{2\omega_{m,\mathbf{q}}^2} |h_{\mathbf{k},\mathbf{k}'}(m,\mathbf{q})|^2 \delta(E_{\mathbf{k}})\, \delta(E_{\mathbf{k}'}) \quad (20)$$

where $\omega_{m,\boldsymbol{q}}$ is the vibrational frequency of the mth phonon mode of wave vector $\mathbf{q}$; $h_{\mathbf{k},\mathbf{k}'}$ is the corresponding electron−phonon matrix element between the electronic states of wave vectors $\mathbf{k}$ and $\mathbf{k}'$; $E_{\mathbf{k}}$ and $E_{\mathbf{k}'}$ are the corresponding energies measured from the energy level of the excited electronic states at the equilibrium structures of the ground states (original point in Figure 2b) of phenanthrene-edge-type hydrocarbons; and $N(0)$ is the total density of states (DOS) per spin. The excited electronic states in phenanthrene-edge-type hydrocarbon crystals are essentially composed of the excited electronic states at the equilibrium structures of the ground states in phenanthrene-dge-type hydrocarbons, and we can write in the form of a Bloch sum

$$\psi(\mathbf{k}) = \frac{1}{\sqrt{N}} \sum_{\mathbf{R}} c(\mathbf{k}) \mathrm{e}^{\mathrm{i}\mathbf{k}\mathbf{R}} \phi_{\mathbf{R}} \quad (21)$$

where $\mathbf{R}$ denotes the cell position; N is the number of molecules in the crystal; and $\phi_{\mathbf{R}}$ is wave function that denotes the excited electronic states for the equilibrium structures of the ground state of phenanthrene-edge-type hydrocarbons at cell position $\mathbf{R}$. If we neglect the intermolecular electron−lattice coupling, then $h_{\mathbf{k},\mathbf{k}'}$ can be reduced to

$$h_{\mathbf{k},\mathbf{k}'}(m,\mathbf{q}) = \langle \psi(\mathbf{k}) | h | \psi(\mathbf{k}') \rangle = \frac{1}{N} \sum_{\mathbf{R}} c^*(\mathbf{k})\, c(\mathbf{k}') \mathrm{e}^{\mathrm{i}(\mathbf{k}-\mathbf{k}')\mathbf{R}} h_{\mathbf{R},\mathbf{R}}(m,\mathbf{q}) \quad (22)$$

where $h_{\mathbf{R},\mathbf{R}}$ is the intramolecular coupling matrix and

$$h_{\mathbf{R},\mathbf{R}}(m,\mathbf{q}) = \langle \phi_{\mathbf{R}} | h | \phi_{\mathbf{R}} \rangle \quad (23)$$

For the one-phonon mode with wave vector $\mathbf{q}$, this term takes the following form:

$$h_{\mathbf{R},\mathbf{R}}(m,\mathbf{q}) = \left(\frac{1}{\sqrt{N}}\right) \mathrm{e}^{\mathrm{i}\mathbf{q}\mathbf{R}} h_{00m} \quad (24)$$

We insert eq 24 in eq 22 taking the condition $\mathbf{k}' = \mathbf{k} - \mathbf{q}$ into account to get

$$h_{\mathbf{k}\mathbf{k}-\mathbf{q}} = \frac{1}{\sqrt{N}} h_{00m} c^*(\mathbf{k})\, c(\mathbf{k}-\mathbf{q}) \quad (25)$$

We now proceed to calculate λ_m by inserting eq 25 in eq 20 considering that $\omega_{m,\mathbf{q}}$ is independent of $\mathbf{q}$. We then obtain

$$\lambda_m = \frac{2}{N(0)} \sum_{\mathbf{k},\mathbf{k}-\mathbf{q}} \frac{1}{2\omega_{m,\mathbf{q}}^2} \frac{h_{00m} h_{00m}^*}{N} \times c^*(\mathbf{k})\, c(\mathbf{k})\, c^*(\mathbf{k}-\mathbf{q})\, c(\mathbf{k}-\mathbf{q})\, \delta(E_{\mathbf{k}})\, \delta(E_{\mathbf{k}-\mathbf{q}}) \quad (26)$$

The partial DOS per molecule at the energy level of the excited electronic state at the equilibrium structure of the ground state of phenanthrene-edge-type hydrocarbons, $n(0)$, can be rewritten as

$$n(0) = \frac{1}{N} \sum_{\mathbf{k}} c^*(\mathbf{k})\, c(\mathbf{k})\, \delta(E_{\mathbf{k}}) \quad (27)$$

We can derive eq 28 from eqs 26 and 27 using $n(0) = N(0)/N$,

$$\lambda_m = \frac{2}{n(0)} \frac{1}{2\omega_m^2} h_{00m} h_{00m}^* n(0)^2 \quad (28)$$

where $n(0)$ is now the DOS per spin and per phenanthrene-edge-type hydrocarbons molecule. λ_m takes the form of eq 29

$$\lambda_m = n(0) \frac{h_{00m}^2}{\omega_m^2} \quad (29)$$

where

$$h_{00m} = h_{A_1} m' \quad (30)$$

Here $h_{A_1 m}'$ is the derivative matrix of the vibronic coupling matrix, $h_{A_1 m}$, derived from eq 32 with respect to the mode amplitude, $Q_{A_1 m}$, as

$$h_{A_1 m}' = \frac{\partial}{\partial Q_{A_1 m}} [A_m Q_{A_1 m}] = \frac{\partial}{\partial Q_{A_1 m}} h_{A_1 m} \quad (31)$$

where

$$h_{A_1 m} = A_m Q_{A_1 m} \quad (32)$$

and A_m is the reduced matrix element and is the slope of the original point (i.e., equilibrium structures of the ground states of phenanthrene-edge-type hydrocarbons ($Q_{A_1 m} = 0$)) on the potential energy surface of the excited B_2 electronic state along each vibrational mode (Figure 2b) and is defined as

$$A_m = \left\langle B_2 \left| \left| \left(\frac{\partial h}{\partial Q_{A_1 m}} \right)_0 \right| \right| B_2 \right\rangle \quad (33)$$

Because $h_{00m}^2 = A_m^2$, one can rewrite eq 28 as

$$\lambda_m = n(0) \frac{A_m^2}{\omega_m^2} \quad (34)$$

Using eqs 6−10 and 33 and after some simple transformations, we finally get the relation between the nondimensional electron−phonon coupling constant, λ_m, and the intramolecular vibronic coupling constant, $g_{B_2(\mathrm{HOMO}\rightarrow\mathrm{LUMO})}(\omega_m)$, as

$$\lambda_m = n(0)\, l_{B_2(\mathrm{HOMO}\rightarrow\mathrm{LUMO})}(\omega_m) \quad (35)$$

where $l_{B_2(\mathrm{HOMO}\rightarrow\mathrm{LUMO})}(\omega_m)$ is the electron−phonon coupling constant defined as

$$l_{B_2(\mathrm{HOMO}\rightarrow\mathrm{LUMO})}(\omega_m) = g_{B_2(\mathrm{HOMO}\rightarrow\mathrm{LUMO})}^2(\omega_m) \hbar\omega_m \quad (36)$$

Electron−Phonon Coupling Constants. We calculated first-order derivatives for the equilibrium structure on each orbital energy surface by distorting the molecule along the A_1 modes of **3ph** using the hybrid Hartree−Fock (HF)/density functional theory (DFT) method of Becke[36] and Lee, Yang, and Parr (B3LYP)[37] and the 6-31G* basis set.[38] The Gaussian 98 program package[39] was used for our theoretical analyses. What we obtained from the first-order derivatives are the dimensionless diagonal linear orbital vibronic coupling constants $g_{\mathrm{LUMO}}(\omega_m)$ and $g_{\mathrm{HOMO}}(\omega_m)$. From these values, we can roughly estimate the vibronic coupling constants $g_{B_2(\mathrm{HOMO}\rightarrow\mathrm{LUMO})}(\omega_m)$ of the A_1 modes to the excited B_2 electronic states in **3ph**. We can estimate the electron−phonon coupling constants $l_{B_2(\mathrm{HOMO}\rightarrow\mathrm{LUMO})}(\omega_m)$ from the dimensionless vibronic coupling constants $g_{B_2(\mathrm{HOMO}\rightarrow\mathrm{LUMO})}(\omega_m)$ in phenanthrene-edge-type hydrocarbons by using eq 36. The calculated electron−phonon coupling constants for the monoanion, monocation, and excited electronic states of **3ph** are shown in Figure 4. Let us take a look at the electron−phonon coupling of the totally symmetric vibrational modes to the excited electronic states of **3ph**. We can see from this Figure that the C−C stretching A_1 modes of 1434 and 1670 cm^{-1} and the low-frequency A_1 mode of 413 cm^{-1} strongly couple to the excited B_2 electronic state of **3ph**. Similar discussions can be made for **4ph** and **5ph**; the C−C stretching modes around 1500 cm^{-1} and the vibronic active modes with frequencies lower than 500 cm^{-1} afford large electron−phonon coupling constants.

Let us next compare the electron−phonon interactions in the excited electronic states with those in the electronic states of the monoanions and cations of phenanthrene-edge-type hydrocarbons.[29] We can see from Figure 4 that the C−C stretching modes around 1500 cm^{-1} and the low-frequency modes around 500 cm^{-1} play an essential role in the electron−phonon interaction in the monoanion and cation of **3ph**. It should be noted that the C−C stretching modes around 1500 cm^{-1} afford larger electron−phonon coupling constants in the excited electronic states than in the electronic states of the monoanion and cation of **3ph**, whereas most of the vibrational modes with frequencies lower than 1000 cm^{-1}, except for the 413 cm^{-1} mode, afford smaller electron−phonon coupling constants in the excited electronic states than in the electronic states of the monoanions. This can be understood as follows. The selected A_1 vibrational modes of **3ph** are shown in Figure 5. We can see from this Figure that carbon atoms are directly distorted toward the direction of the neighboring carbon atoms in the C−C stretching modes of 1434 and 1670 cm^{-1}. Also, there are complete phase pattern differences between the HOMO and LUMO; the atomic orbitals between C_1 and C_2 atoms, between C_3 and C_4 atoms, between C_3 and C_8 atoms, between C_4 and C_5 atoms, between C_6 and C_7 atoms, and between C_8 and C_9 atoms in the HOMO (LUMO) are combined in phase (out of phase), and those between C_2 and C_3 atoms, between C_5 and C_6 atoms, and between C_7 and C_8 atoms in the HOMO (LUMO) are combined out of phase (in phase). That is, the atomic orbitals

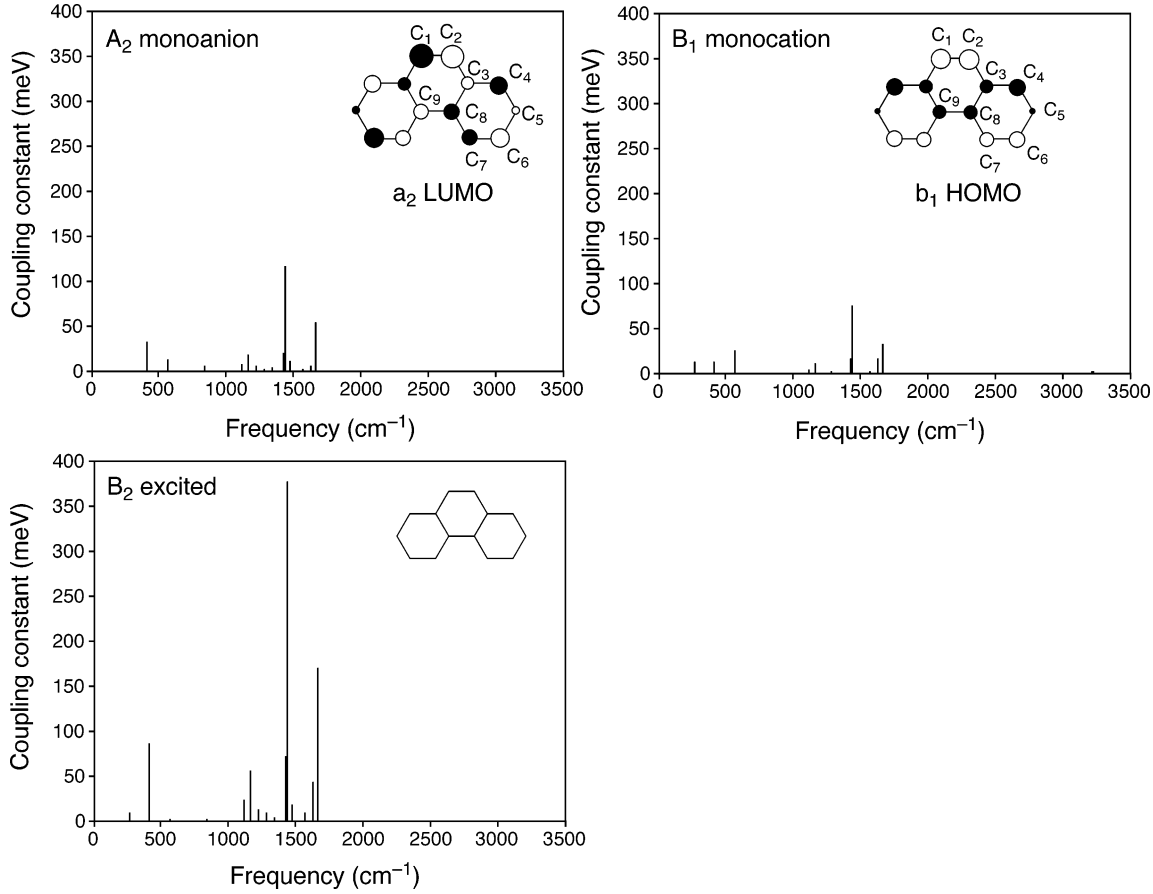

Figure 4. Electron-phonon coupling constants for the negatively, positively, and excited electronic states of phenanthrene-edge-type hydrocarbons.

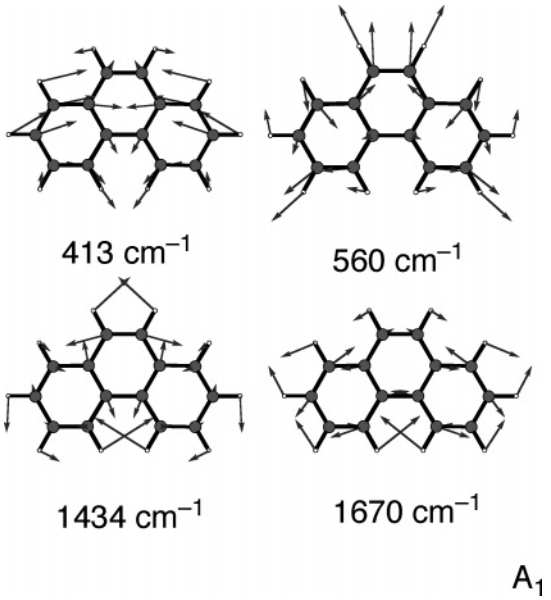

Figure 5. Selected vibronic active modes of phenanthrene.

between two neighboring carbon atoms that are combined in phase (out of phase) in the HOMO are combined out of phase (in phase) in the LUMO in **3ph**. When **3ph** is distorted along the A_1 mode of 1434 cm^{-1} toward the same direction as shown in the Figure, the bonding (antibonding) interactions between C_1 and C_2 atoms and between C_3 and C_8 atoms in the HOMO (LUMO) become weaker, and the antibonding (bonding) interactions between C_2 and C_3 atoms in the HOMO (LUMO) become stronger. Therefore, the HOMO (LUMO) is significantly destabilized (stabilized) in energy by such a distortion. In a similar way, when **3ph** is distorted along the A_1 mode of 1670 cm^{-1}, the bonding (antibonding) interactions between two neighboring carbon atoms in the HOMO (LUMO) become stronger, and the antibonding (bonding) interactions between them in the HOMO (LUMO) become weaker. Therefore, the HOMO (LUMO) is significantly stabilized (destabilized) in energy by such a distortion. That is, the strengths of the orbital interactions between two neighboring carbon atoms, the change of which make the vibronic interaction properties completely different between the HOMO and LUMO, significantly change, and the HOMO is stabilized (destabilized) in energy when the LUMO is destabilized (stabilized). In such cases, vibronic interactions in the excited electronic states are significantly strengthened by the vibronic interaction effects originating from the stabilized (destabilized) LUMO and the destabilized (stabilized) HOMO as shown in Figure 3d-i. This is the reason that the C−C stretching modes around 1500 cm^{-1} afford larger electron−phonon coupling constants in the excited B_2 electronic state of **3ph** than in the electronic states in the monoanion and cation of **3ph**.

Let us next look into the electron−phonon coupling of the A_1 frequency modes whose frequencies are lower than 1000 cm^{-1} to the excited B_2 electronic state of **3ph**. For example, in low-frequency modes such as the A_1 mode of 560 cm^{-1}, which are analogous to the acoustic modes of phonons in solids, two neighboring carbon atoms move in similar directions. Therefore, the strengths of the orbital interactions between two neighboring carbon atoms, the change of which make the vibronic interaction properties significantly different between the HOMO and LUMO, do not significantly change. And such displacements of carbon atoms change the strengths of orbital interactions between the two neighboring carbon atoms in the HOMO and

TABLE 1: Necessary Minimum $n(0)$ Values as a Function of μ^* that Satisfy Equation 39 ($-\lambda_m + \mu^* \leq 0$)[a]

	$\mu^* = 0.1$	$\mu^* = 0.2$	$\mu^* = 0.3$	$\mu^* = 0.4$	$\mu^* = 0.5$	$\mu^* = 0.6$	$\mu^* = 0.7$	$\mu^* = 0.8$
3ph$^-$	0.862	1.724	2.586	3.448	4.310	5.172	6.034	6.897
3ph$^+$	1.333	2.667	4.000	5.333	6.667	8.000	9.333	10.667
3ph^{excited}	0.265	0.531	0.796	1.061	1.326	1.592	1.857	2.122
4ph$^-$	1.695	3.390	5.085	6.780	8.475	10.169	11.864	13.559
4ph$^+$	2.941	5.882	8.824	11.765	14.706	17.647	20.588	23.529
4ph^{excited}	0.549	1.099	1.648	2.198	2.747	3.297	3.846	4.396
5ph$^-$	2.941	5.882	8.824	11.765	14.706	17.647	20.588	23.529
5ph$^+$	5.882	11.765	17.647	23.529	29.412	35.294	41.176	47.059
5ph^{excited}	1.010	2.020	3.030	4.040	5.051	6.060	7.071	8.081

[a] As an example, the C−C stretching modes of 1434, 1409, and 1396 cm^{-1} for **3ph**, **4ph**, and **5ph**, respectively, are considered.

LUMO in a similar manner; the LUMO is also stabilized (destabilized) in energy when the HOMO is stabilized (destabilized) in energy. In such cases, vibronic interactions in the excited B_2 electronic states are weakened by the compensation of the vibronic interaction effects originating from the HOMO and LUMO as shown in Figure 3d-ii. Similar discussions can be made for the other A_1 modes with frequencies lower than 1000 cm^{-1}, except for the 413 cm^{-1}mode. This is the reason that the low-frequency A_1 modes afford smaller electron−phonon coupling constants in the excited B_2 electronic state than in the electronic state in the monoanion of **3ph**. Similar discussions can be made for **4ph** and **5ph**; the C−C stretching modes around 1500 cm^{-1} (the vibrational modes with frequencies lower than 1000 cm^{-1}) afford larger (smaller) electron−phonon coupling constants in the excited electronic states than in the electronic states of the monoanions.

In summary, the complete phase pattern difference between the HOMO and the LUMO (the atomic orbitals between two neighboring carbon atoms combined in phase (out of phase) in the HOMO are combined out of phase (in phase) in the LUMO) is the main reason that the C−C stretching modes around 1500 cm^{-1} afford much larger electron−phonon coupling constants in the excited electronic states than in the charged electronic states. In this study, we consider only phenanthrene-edge-type hydrocarbons as an example. However, considering that an optically allowed transition is allowed in the case in which an electron in the symmetric (antisymmetric) occupied orbitals is promoted to the antisymmetric (symmetric) unoccupied orbitals, the electron−phonon interactions can generally be expected to be much stronger in photoinduced excited electronic states than in charged electronic states in various molecular systems as well as in phenanthrene-edge-type hydrocarbons.

Possible Electron Pairing in the Photoinduced Excited Electronic States in Phenanthrene-Edge-Type Hydrocarbons. Once the attractive interaction between two electrons dominates the repulsive screened Coulomb interaction as expressed by eqs 37 and 38, the system would produce as many Cooper pairs as possible to lower its energy.

$$V_{\text{int}}^{(i,j)} = -l_{\text{B(HOMO}\rightarrow\text{LUMO)}} + V_{i,j}^{\text{Coulomb}} < -l_{\text{B(HOMO}\rightarrow\text{LUMO)}}(\omega_m) + V_{i,j}^{\text{Coulomb}} < 0 \quad (37)$$

and

$$-\lambda + \mu^* = -n(0)\, l_{\text{B(HOMO}\rightarrow\text{LUMO)}} + \mu^* < -n(0)\, l_{\text{B(HOMO}\rightarrow\text{LUMO)}}(\omega_m) + \mu^* < 0 \quad (38)$$

where the λ is the dimensionless total electron−phonon coupling constant, $l_{\text{B(HOMO}\rightarrow\text{LUMO)}}$ is the total electron−phonon coupling constant,[13−15,29] and μ^* is the Coulomb pseudopotential usually used as a fitting parameter, which ranges from about 0.10−0.20 in conventional superconductivity. The $n(0)$ values as a function of μ^* under which $\lambda_m = \mu^*$ is satisfied are listed in Table 1. For example, considering the large $l_{\text{B(HOMO}\rightarrow\text{LUMO)}}(\omega_m)$ value (0.377 eV) for the C−C stretching mode of 1434 cm^{-1} and the usual μ^* values (∼0.20), eq 40 is satisfied if $n(0) \geq 0.531$ for **3ph**. Therefore, we can expect that the attractive interaction between two electronic states can dominate the repulsive screened Coulomb interaction between two electronic states on separate molecules more easily in photoinduced excited electronic states than in charged electronic states in molecular systems.

Conduction electrons are subject to the Pauli exclusion principle. Condensation into a zero-momentum state may be realized if the two (four) electrons form a bound state via the attractive electron−electron interaction and the resulting pair of electrons behaves as a single particle obeying Bose statistics in the monoanions and cations (the excited electronic states).

Let us first look into the possible electron pairing in the negatively charged molecular systems. Possible electron pairing between electrons with discrete wave vectors on separate molecules is shown in Figure 6. It should be noted here that this Figure describes the coordinate space pairing of electrons expressed by $\Phi(\mathbf{r}_{\text{LUMO},i}, \mathbf{r}_{\text{LUMO},j})$, $\Phi(\mathbf{r}_{\text{HOMO},i}, \mathbf{r}_{\text{HOMO},j})$, and $\Phi(\mathbf{r}_{\text{HO}\rightarrow\text{LU},i}, \mathbf{r}_{\text{HO}\rightarrow\text{LU},j})$ for the monoanions, monocations, and the excited electronic states, respectively. However, to show the electronic states in each molecule in detail, the state vectors in the momentum space of each molecule are also shown in this Figure. As can be seen in Figure 6a, it has generally been considered that the possibility of electron pairing is that between two electrons with opposite discrete molecular wave vectors $\pm\mathbf{k}_{\text{LUMO},j}$ and opposite spins in negatively charged molecular systems. Thus, we have thought that intermolecular electron pairing can occur between two electronic states with opposite molecular wave vectors and opposite spins on separate molecules, as shown in Figure 6a. In a similar way, it can be considered that the possibility of electron pairing is that between two electrons with opposite discrete molecular wave vectors $\pm\boldsymbol{k}_{\text{HOMO},j}$ and opposite spins in positively charged molecular systems. By analogy to the BCS theory, the wave function in the monoanion is constructed by taking a linear combination of many normal-state configurations in which the Bloch states are occupied by a pair of opposite momenta and spins.

$$\Phi(\mathbf{r}_{\text{LUMO},i}, \mathbf{r}_{\text{LUMO},j}) = \sum_{i,j}\sum_{s=\pm 1/2} a_{ij}\Phi(+\mathbf{k}_{\text{LUMO},i,s}, -\mathbf{k}_{\text{LUMO},j,-s}) \quad (39)$$

where $|a_{ij}|^2$ represents the probability of finding a pair of electrons with states $+\boldsymbol{k}_{\text{LUMO},i,s}$ and $-\boldsymbol{k}_{\text{LUMO},j,-s}$. A Cooper pair is expressed by the wave function in eq 39. Therefore, it is important to realize that each Cooper pair is composed of the

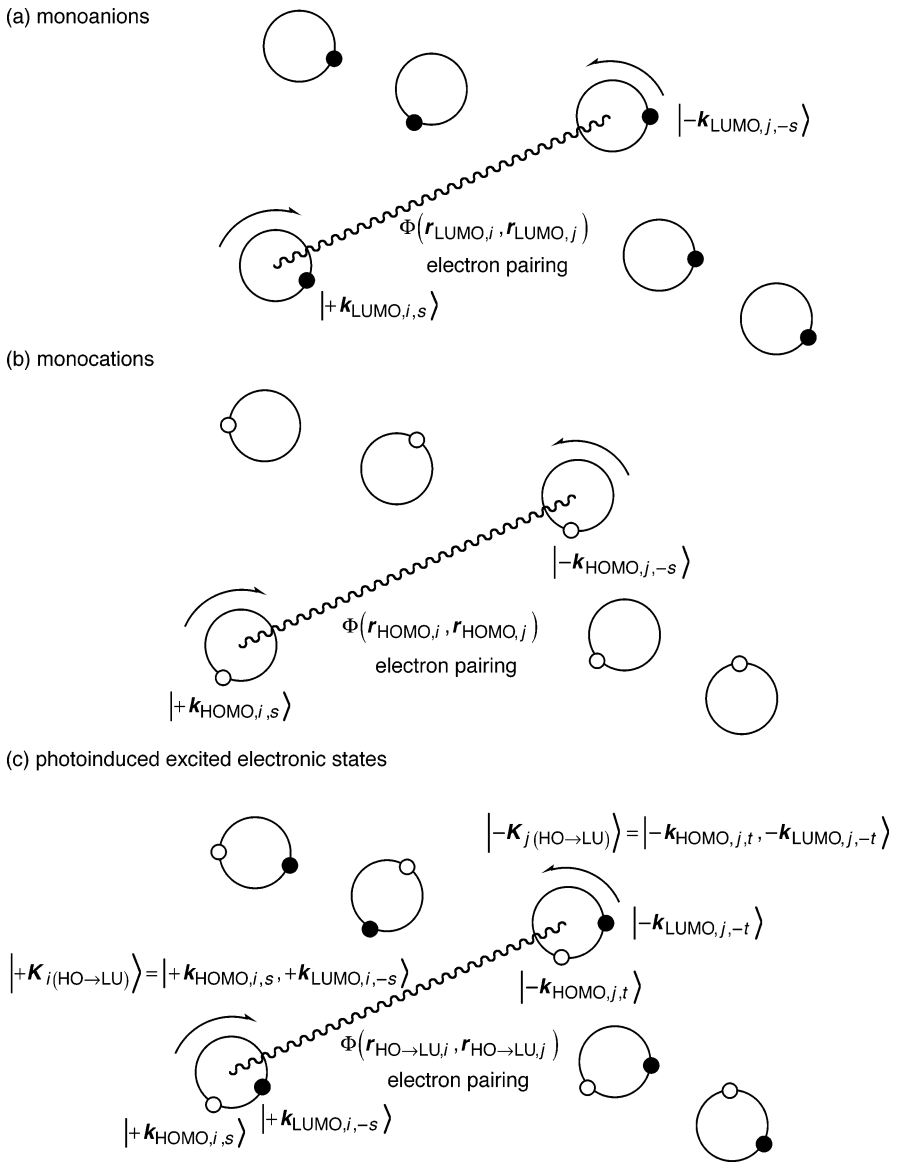

Figure 6. Electron pairing between electrons with discrete wave vectors on separate molecules. The closed and opened circles denote the electrons partially occupying the LUMO and HOMO, respectively, in each molecule.

Bloch states with all possible wave vectors $+\boldsymbol{k}_{\mathrm{LUMO},i}$. In a similar way, which can be defined in the case of the monocations (Figure 6b),

$$\Phi(\mathbf{r}_{\mathrm{HOMO},i}, \mathbf{r}_{\mathrm{HOMO},j}) = \sum_{i,j} \sum_{s=\pm 1/2} a_{ij} \Phi(+\mathbf{k}_{\mathrm{HOMO},i,s}, -\mathbf{k}_{\mathrm{HOMO},j,-s}) \quad (40)$$

Let us next consider electron pairing of the molecular systems in the photoinduced excited electronic states. A possibility of electron pairing is that between two electronic states with opposite discrete molecular wave vectors $\pm\mathbf{K}_j$ and opposite spins, as shown in Figure 6c. The wave function denoting the pair of electrons in the excited electronic states can be defined as

$$\begin{aligned}\Phi(\mathbf{r}_{\mathrm{HO}\rightarrow\mathrm{LU},i}, \mathbf{r}_{\mathrm{HO}\rightarrow\mathrm{LU},j}) &= \sum_{i,j}\sum_{S} a_{ij} \Phi(+\mathbf{K}_{i(\mathrm{HO}\rightarrow\mathrm{LU}),S}, -\mathbf{K}_{j(\mathrm{HO}\rightarrow\mathrm{LU}),-S}) \\ &= \sum_{i,j} \sum_{s,t=\pm 1/2} a_{ij} \Phi(+\mathbf{k}_{\mathrm{HOMO},i,s}, + \mathbf{k}_{\mathrm{LUMO},i,-s}, -\mathbf{k}_{\mathrm{HOMO},j,t}, -\mathbf{k}_{\mathrm{LUMO},j,-t}) \quad (41)\end{aligned}$$

Once the attractive interaction between two electrons dominates the repulsive screened Coulomb interaction, the system would produce as many Cooper pairs as possible to lower its energy. The ground-state wave function in the superconducting state by using a Hartree-like approximation can be constructed and expressed as a product of the individual Cooper pair wave functions given by eqs 42 and 43:

$$\begin{aligned}\psi_0(\mathbf{r}_1, \mathbf{r}_2, ..., \mathbf{r}_{n_0}) &= \sum_{\sigma} (\mathrm{sgn}\sigma) \sum \Phi(\mathbf{r}_1, \mathbf{r}_2)\, \Phi(\mathbf{r}_3, \mathbf{r}_4) ... \Phi(\mathbf{r}_{n-1}, \mathbf{r}_n) \\ &= \sum_{\sigma} (\mathrm{sgn}\sigma) \sum \prod_{i,j(i\neq j)}^{n} \Phi(\mathbf{r}_i, \mathbf{r}_j) \quad (42)\end{aligned}$$

where n is the total number of electrons participating in the superconducting, $\mathbf{r}_i$ is the position coordinate of the ith electron, the Φ's on the right-hand side are the same for all pairs, and the summation in eq 42 means that all possible two-electron pairings for n electrons such as $\Phi(\mathbf{r}_1, \mathbf{r}_2)\, \Phi(\mathbf{r}_3, \mathbf{r}_4) ... \Phi(\mathbf{r}_{n-1}, \mathbf{r}_n) + \Phi(\mathbf{r}_1, \mathbf{r}_3)\, \Phi(\mathbf{r}_2, \mathbf{r}_4) ... \Phi(\mathbf{r}_{n-1}, \mathbf{r}_n) + ...$ are considered. Furthermore, σ denotes permutations of two electrons such as

1 and 2, 3 and 4, i and j, and so on, and (sgnσ) denotes $+1$ (-1) in the case in which such permutations are performed an even (odd) number of times because the wave function should be antisymmetric with respect to any permutations of two electrons. In a similar way, that for the excited electronic states is defined as

$$\psi_0(\mathbf{r}_1, \mathbf{r}_2,...,\mathbf{r}_{n_0}) = \sum_{\sigma}(\mathrm{sgn}\sigma) \sum \Phi(\mathbf{r}_1, \mathbf{r}_2; \mathbf{r}_3, \mathbf{r}_4)\, \Phi(\mathbf{r}_5, \mathbf{r}_6; \mathbf{r}_7, \mathbf{r}_8)...\Phi(\mathbf{r}_{n-3}, \mathbf{r}_{n-2}; \mathbf{r}_{n-1}, \mathbf{r}_n) = \sum_{\sigma}(\mathrm{sgn}\sigma) \sum \prod_{i,j,k,l(i\neq j\neq k\neq l)}^{n} \Phi(\mathbf{r}_i, \mathbf{r}_j; \mathbf{r}_k, \mathbf{r}_l) \quad (43)$$

The square of the many-electron wave function in eqs 42 and 43 gives the probability of finding superconducting electrons at $\mathbf{r}_1$, $\mathbf{r}_2$,..., $\mathbf{r}_{n_0}$ regardless of their momenta. The Cooper pair $\Phi(\mathbf{r}_i, \mathbf{r}_j)$ involved in eq 42 and pair $\Phi(\mathbf{r}_i, \mathbf{r}_j; \mathbf{r}_k, \mathbf{r}_l)$ in eq 43 can be regarded as a single particle obeying Bose−Einstein statistics. Because of their resultant zero spin, such (Cooper) pairs can behave as Bose particles, and because of the resultant zero momentum, the system is in an ordered state.

The superconducting state is in a constrained condition such that we cannot alter the momentum of the paired electrons at will. As a consequence, for the paired electrons, the scattering that changes the direction of the wave vector is prohibited. Once a current is induced, the same velocity vector **v** that is parallel to the applied field is acquired by each (Cooper) pair. Thus, the drift velocity of all (Cooper) pairs becomes **v**. Thus, all (Cooper) pairs acquire the same momentum. Such a current flowing without disturbing the ordered state results in a resistanceless conduction.

In the monoanions, the partially occupied conduction band is mainly formed by the LUMO of each molecule, and in the monocations, the partially occupied valence band is mainly formed by the HOMO of each molecule. However, in the excited electronic states, electrons partially occupying the valence band formed by the HOMO of each molecule as well as those partially occupying the conduction band formed by the LUMO of each molecule play an essential role in the electrical conductivity. Considering that the $l_{\mathrm{B(HOMO\rightarrow LUMO)}}(\omega_m)$ values around 1500 cm^{-1} are much larger than the $l_{\mathrm{LUMO}}(\omega_m)$ and $l_{\mathrm{HOMO}}(\omega_m)$ values, we can expect the photoinduced excited electronic states to exhibit much higher temperature superconductivity than the monoanions and cations in nanosized molecular systems on the basis of the hypothesis that the vibronic interactions between the intramolecular vibrations and the electronic states play an essential role in the occurrence of possible superconductivity in nanosized molecular systems. However, it should be noted that the strong electron−phonon coupling is favorable for Cooper pair formation but at the same time it contributes to the relaxation of the excited states. Because of such competition between these two processes, we cannot rule out the possibility that the relaxation of the excited states occurs before the electron pairs are formed. Even though it may be very difficult for such photoinduced excited electronic states of molecular systems to exhibit superconductivity because of the unstable electronic structures of the excited electronic states mentioned above, the technological difficulties encountered up until now, and, furthermore, the $l_{\mathrm{B(HOMO\rightarrow LUMO)}}(\omega_m)$ values that would be somewhat overestimated because of one-electron approximations in eqs 9 and 10, it is worth noting that the C−C stretching modes around 1500 cm^{-1} afford much larger electron−phonon coupling constants in the excited electronic states than in the charged electronic states because of the complete phase pattern difference between the HOMO and the LUMO. (The atomic orbitals between two neighboring carbon atoms combined in phase (out of phase) in the HOMO are combined out of phase (in phase) in the LUMO.)

Concluding Remarks

We studied electron−phonon interactions in the photoinduced excited electronic states in molecular systems such as phenanthrene-edge-type hydrocarbons and compared these calculated results with those for the monoanions and cations. The C−C stretching modes around 1500 cm^{-1} and the low-frequency modes with frequencies lower than 500 cm^{-1} strongly couple to the excited electronic states of phenanthrene-edge-type hydrocarbons. The $l_{\mathrm{B(HOMO\rightarrow LUMO)}}(\omega_m)$ values around 1500 cm^{-1} are much larger than the $l_{\mathrm{LUMO}}(\omega_m)$ and $l_{\mathrm{HOMO}}(\omega_m)$ values around 1500 cm^{-1} in phenanthrene-edge-type hydrocarbons. This is because the C−C stretching modes around 1500 cm^{-1} afford much larger electron−phonon coupling constants in the excited electronic states than in the electronic states of the monoanions and cations, whereas most of the vibrational modes with frequencies lower than 1000 cm^{-1} afford slightly smaller electron−phonon coupling constants in the excited electronic states than in the electronic states of the monoanions in phenanthrene-edge-type hydrocarbons. This can be understood in view of the orbital patterns of the frontier orbitals in phenanthrene-edge-type hydrocarbons as follows. There are complete phase pattern differences between the HOMO and LUMO; the atomic orbitals between two neighboring carbon atoms that are combined in phase (out of phase) in the HOMO are combined out of phase (in phase) in the LUMO in phenanthrene-edge-type hydrocarbons. For example, when **3ph** is distorted along the A_1 mode of 1434 cm^{-1}, the bonding (antibonding) interactions between two neighboring carbon atoms in the HOMO (LUMO) become weaker, and the antibonding (bonding) interactions between them in the HOMO (LUMO) become stronger. Therefore, the HOMO (LUMO) is significantly destabilized (stabilized) in energy by such a distortion. That is, the strengths of the orbital interactions between two neighboring carbon atoms, the changes of which make the vibronic interaction properties completely different between the HOMO and LUMO, significantly change, and the HOMO is stabilized (destabilized) in energy when the LUMO is destabilized (stabilized). In such cases, vibronic interactions in the excited electronic states are significantly strengthened by the vibronic interaction effects originating from the stabilized (destabilized) LUMO and the destabilized (stabilized) HOMO. This is the reason that the C−C stretching modes around 1500 cm^{-1} afford larger electron−phonon coupling constants in the excited electronic states than in the monoanions and cations in phenanthrene-edge-type hydrocarbons. However, in low-frequency modes such as the A_1 mode of 560 cm^{-1}, which are analogous to acoustic modes of phonons in solids, two neighboring carbon atoms move in similar directions. Therefore, the strengths of the orbital interactions between two neighboring carbon atoms, the change of which make the vibronic interaction properties significantly different between the HOMO and LUMO, do not change significantly. Also, such displacements of carbon atoms change the strengths of orbital interactions between the two neighboring carbon atoms in the HOMO and LUMO in a similar manner; the HOMO is also stabilized (destabilized) in energy when the LUMO is stabilized (destabilized). In such cases, vibronic interactions in the excited B_2 electronic states are weakened by the compensation of the

vibronic interaction effects originating from the HOMO and LUMO. This is the reason that the electron−phonon coupling constants for the vibrational modes with frequencies lower than 1000 cm^{-1} are slightly smaller in the excited electronic states than in the monoanions and cations in phenanthrene-edge-type hydrocarbons.

We also discussed the possible electron pairing and Bose−Einstein condensation in these electronic states. In the case of monoanions and cations, we have considered that electrons partially occupying the conduction band and partially occupying the valence band, formed by the LUMO and the HOMO of each molecule, respectively, play an essential role in the electrical conductivity. However, we consider the electron−phonon interactions in the excited electronic states in this study, in which electrons partially occupying the valence band as well as partially occupying the conduction band formed by the HOMO and LUMO of each molecule, respectively, play an essential role in the electron−phonon interactions and in electrical conductivity. The strong coupling is favorable for Cooper pair formation, but at the same time it contributes to the relaxation of the excited states. Because of such competition of these two processes, we cannot rule out the possibility that the relaxation of the excited states occurs before the electron pairs are formed. Even though it may be very difficult for the excited electronic states of molecular systems to exhibit superconductivity because of unstable electronic states of the excited electronic states and the technological difficulties encountered up until now, it is worth noting that the C−C stretching modes around 1500 cm^{-1} afford much larger electron−phonon coupling constants in the excited electronic states than in the charged electronic states in phenanthrene-edge-type hydrocarbons because of the complete phase pattern difference between the HOMO and the LUMO. (The atomic orbitals between two neighboring carbon atoms combined in phase (out of phase) in the HOMO are combined out of phase (in phase) in the LUMO.) In this study, we consider only phenanthrene-edge-type hydrocarbons as an example. However, considering that optically allowed transitions are allowed in cases in which an electron in the symmetric (antisymmetric) occupied orbitals is promoted to the antisymmetric (symmetric) unoccupied orbitals, the electron−phonon interactions can generally be expected to be much stronger in photoinduced excited electronic states than in charged electronic states in various molecular systems as well as in phenanthrene-edge-type hydrocarbons.

Acknowledgment. This study was performed under the project of the Academic Frontier Center at Nagasaki Institute of Applied Science. This work is partially supported by a Grant-in-Aid for Scientific Research from the Japan Society for the Promotion of Science (JSPS-15350114, JSPS-16560618).

References and Notes

(1) Jahn, H. A.; Teller, E. *Proc. R. Soc. London, Ser. A* **1937**, *161*, 220.

(2) Kivelson, S.; Heeger, A. J. *Synth. Met.* **1988**, *22*, 371.

(3) (a) Bersuker, I. B. *The Jahn−Teller Effect and Vibronic Interactions in Modern Chemistry*; Plenum: New York, 1984. (b) Bersuker, I. B.; Polinger, V. Z. *Vibronic Interactions in Molecules and Crystals*; Springer: Berlin, 1989. (c) Bersuker, I. B. *Chem. Rev.* **2001**, *101*, 1067.

(4) Grimvall, G. *The Electron−Phonon Interaction in Metals*; North-Holland: Amsterdam, 1981.

(5) (a) Schrieffer, J. R. *Theory of Superconductivity*; Addison-Wesley: Reading, MA, 1964. (b) de Gennes, P. G. *Superconductivity of Metals and Alloys*; Benjamin: New York, 1966. (c) Mizutani, U. *Introduction to the Electron Theory of Metals*; Cambridge University Press: Cambridge, U.K., 1995.

(6) (a) Kittel, C. *Quantum Theory of Solids*; Wiley: New York, 1963. (b) Ziman, J. M. *Principles of the Theory of Solids*; Cambridge University: Cambridge, U.K., 1972. (c) Ibach, H.; Lüth, H. *Solid-State Physics*; Springer: Berlin, 1995.

(7) Little, W. A. *Phys. Rev. A*, **1964**, *134*, 1416.

(8) (a) Jérome, D.; Mazaud, A.; Ribault, M.; Bechgaad, K. *J. Phys. Lett.* (France) **1980**, *41*, L95. (b) Ribault, M.; Benedek, G.; Jérome, D.; Bechgaad, K. *J. Phys. Lett.* (France) **1980**, *41*, L397. (c) Jérome, D.; Schulz, H. J. *Adv. Phys.* **1982**, *31*, 299. (d) Ishiguro, T.; Yamaji, K. *Organic Superconductors*; Springer: Berlin, 1990. (e) Williams, J. M.; Ferraro, J. R.; Thorn, R. J.; Karlson, K. D.; Geiser, U.; Wang, H. H.; Kini, A. M.; Whangbo, M.-H. *Organic Superconductors*; Prentice Hall: Englewood Cliffs, NJ, 1992.

(9) Oshima, K.; Urayama, H.; Yamochi, H.; Saito, G. *J. Phys. Soc. Jpn.* **1988**, *57*, 730.

(10) (a) Hebard, A. F.; Rosseinsky, M. J.; Haddon, R. C.; Murphy, D. W.; Glarum, S. H.; Palstra, T. T. M.; Ramirez, A. P.; Kortan, A. R. *Nature* **1991**, *350*, 600. (b) Rosseinsky, M. J.; Ramirez, A. P.; Glarum, S. H.; Murphy, D. W.; Haddon, R. C.; Hebard, A. F.; Palstra, T. T. M.; Kortan, A. R.; Zahurak, S. M.; Makhija, A. V. *Phys. Rev. Lett.* **1991**, *66*, 2830.

(11) Tanigaki, K.; Ebbesen, T. W.; Saito, S.; Mizuki, J.; Tsai, J. S.; Kubo, Y.; Kuroshima, S. *Nature* **1991**, *352*, 222.

(12) Palstra, T. T. M.; Zhou, O.; Iwasa, Y.; Sulewski, P. E.; Fleming, R. M.; Zegarski, B. R. *Solid State Commun.* **1995**, *93*, 327.

(13) (a) Varma, C. M.; Zaanen, J.; Raghavachari, K. *Science* **1991**, *254*, 989. (b) Lannoo, M.; Baraff, G. A.; Schlüter, M.; Tomanek, D. *Phys. Rev. B* **1991**, *44*, 12106. (c) Asai, Y.; Kawaguchi, Y. *Phys. Rev. B* **1992**, *46*, 1265. (d) Faulhaber, J. C. R.; Ko, D. Y. K.; Briddon, P. R. *Phys. Rev. B* **1993**, *48*, 661. (e) Antropov, V. P.; Gunnarsson, O.; Lichtenstein, A. I. *Phys. Rev. B* **1993**, *48*, 7651. (f) Gunnarsson, O. *Phys. Rev. B* **1995**, *51*, 3493. (g) Gunnarsson, O.; Handschuh, H.; Bechthold, P. S.; Kessler, B.; Ganteför, G.; Eberhardt, W. *Phys. Rev. Lett.* **1995**, *74*, 1875. (h) Dunn, J. L.; Bates, C. A. *Phys. Rev. B* **1995**, *52*, 5996. (i) Gunnarsson, O. *Rev. Mod. Phys.* **1997**, *69*, 575. (j) Devos, A.; Lannoo, M. *Phys. Rev. B* **1998**, *58*, 8236. (k) Gunnarsson, O. *Nature* **2000**, *408*, 528.

(14) (a) Kato, T.; Yamabe, T. *J. Chem. Phys.* **2001**, *115*, 8592. (b) Kato, T.; Yamabe, T. *Recent Research Developments in Quantum Chemistry*; Transworld Research Network: Kerala, India, 2004. (c) Kato, T.; Yamabe, T. *Recent Research Developments in Physical Chemistry*; Transworld Research Network: Kerala, India, 2004.

(15) (a) Coropceanu, V.; Filho, D. A. da Silva; Gruhn, N. E.; Bill, T. G.; Brédas, J. L. *Phys. Rev. Lett.* **2002**, *89*, 275503. (b) Brédas, J. L.; Beljonne, D.; Coropceanu, V.; Jérome, C. *Chem. Rev.* **2004**, *104*, 4971.

(16) (a) T.; Harada, T.; Tanaka, K.; Yamabe, T. *Synth. Met.* **1994**, *62*, 153. (b) Yata, S.; Hato, Y.; Kinoshita, H.; Ando, N.; Anekawa, A.; Hashimoto, T.; Yamaguchi, M.; Tanaka, K.; Yamabe, T. *Synth. Met.* **1995**, *73*, 273. (c) Wang, S.; Yata, S.; Nagano, J.; Okano, Y.; Kinoshita, H.; Kikuta H.; Yamabe, T. *J. Electrochem. Soc.* **2000**, *147*, 2498.

(17) Whangbo, M.-H.; Hoffmann, R.; Woodward, R. B. *Proc. R. Soc. London, Ser. A* **1979**, *366*, 23.

(18) (a) Kertesz, M.; Hoffmann, R. *Solid State Commun.* **1983**, *47*, 97. (b) Kertesz, M.; Lee, Y. S.; Stewart, J. J. P. *Int. J. Quantum Chem.* **1989**, *35*, 305. (c) Lee, Y. S.; Kertesz, M. *J. Chem. Phys.* **1988**, 2609. (d) Hong, S. Y.; Kertesz, M.; Lee, Y. S.; Kim, O.-K. *Chem. Mater.* **1992**, *4*, 378. (e) Kertesz, M. *Macromolecules* **1995**, *28*, 1475. (f) Kertesz, M.; Ashertehrani, A. *Macromolecules* **1996**, *29*, 940.

(19) (a) Brédas, J. L.; Chance, R. R.; Baughman, R. H.; Silbey, R. *J. Chem. Phys.* **1982**, *76*, 3673. (b) Boudreaux, D. S.; Chance, R. R.; Elsenbaumer, R. L.; Frommer, J. E.; Brédas, J. L. *Phys. Rev. B* **1985**, *31*, 652. (c) Brédas, J. L.; Baughman, R. H. *J. Chem. Phys.* **1985**, *83*, 1316. (d) Toussaint, J. M.; Brédas, J. L. *Synth. Met.* **1992**, *46*, 325.

(20) (a) Klein, D. J.; Alexander, S. A.; Randic, M. *Mol. Cryst. Liq. Cryst.* **1989**, *176*, 109. (b) Klein, D. J. *Rep. Mol. Theory* **1990**, *1*, 91. (c) Klein, D. J. *Chem. Phys. Lett.* **1994**, *217*, 261. (d) Klein, D. J.; Bytautas, L. J. *J. Phys. Chem. A* **1999**, *103*, 5196.

(21) (a) Yamabe, T.; Tanaka, K.; Ohzeki, K.; Yata, S. *Solid State Commun.* **1982**, *44*, 823. (b) Tanaka, K.; Ohzeki, K.; Nankai, S.; Yamabe, T.; Shirakawa, H. *J. Phys. Chem. Solid* **1982**, *44*, 1069. (c) Tanaka, K.; Ueda, K.; Koike, T.; Yamabe, T. *Solid State Commun.* **1984**, *51*, 943. (d) Tanaka, K.; Yamanaka, S.; Ueda, K.; Takeda, S.; Yamabe, T. *Synth. Met.* **1987**, *20*, 333. (e) Tanaka, K.; Murashima, M.; Yamabe, T. *Synth. Met.* **1988**, *24*, 371.

(22) (a) Tyutyulkov, N.; Polansky O. E.; Fabian, J. *Z. Naturforsch.* **1977**, *A32*, 490. (b) Tyutyulkov, N.; Tadjer, A.; Mintsheva, I. *Synth. Met.* **1990**, *38*, 313. (c) Baumgarten, M.; Karabunarliev, S.; Koch, K.-H.; Müllen, K.; Tyutyulkov, N. *Synth. Met.* **1992**, *47*, 21. (d) Reisch, H.; Wiesler, U.; Scherf, U.; Tyutyulkov, N. *Macromolecules* **1996**, *29*, 8204. (e) Tyutyulkov, N.; Madjarova, G.; Dietz, F.; Müllen, K. *J. Phys. Chem. B* **1998**, *102*, 10183.

(23) (a) Nakada, K.; Fujita, M.; Dresselhaus, G.; Dresselhaus, M. S. *Phys. Rev.* **1996**, *B54*, 17954. (b) Fujita, M.; Wakabayashi, K.; Nakada, K.; Kusakabe, K. *J. Phys. Soc. Jpn.* **1996**, *65*, 1920.

(24) Hess, B. A., Jr.; Schaad, L. J. *J. Org. Chem.* **1971**, *36*, 3418.

(25) (a) Stein, S. E.; Brown, R. L. *J. Am. Chem. Soc.* **1987**, *109*, 3721. (b) Chen, R. H.; Kafafi, S. A.; Stein, S. E. *J. Am. Chem. Soc.* **1989**, *111*, 1418. (c) Stein, S. E.; Brown, R. L. *J. Am. Chem. Soc.* **1991**, *113*, 787.

(26) Novák, P.; Müller, K.; Santhanam, K. S. V.; Haas, O. *Chem. Rev.* **1997**, *97*, 207.

(27) (a) Yoshizawa, K.; Okahara, K.; Sato, T.; Tanaka, K.; Yamabe, T. *Carbon* **1994**, *32*, 1517. (b) Yoshizawa, K.; Yahara, K.; Tanaka, K.; Yamabe, T. *J. Phys. Chem. B* **1998**, *102*, 498.

(28) Ago, H.; Nagata, K.; Yoshizawa, K.; Tanaka, K.; Yamabe, T. *Bull. Chem. Soc. Jpn.* **1997**, *70*, 1717.

(29) (a) Kato, T.; Yoshizawa, K.; Hirao, K. *J. Chem. Phys.* **2002**, *116*, 3420. (b) Kato, T.; Yamabe, T. *J. Chem. Phys.* **2004**, *120*, 3311.

(30) Conwell, E. M. *Phys. Rev. B* **1980**, *22*, 1761.

(31) Kato, T.; Yoshizawa, K.; Yamabe, T. *J. Chem. Phys.* **2000**, *113*, 2188.

(32) (a) Squire, R. H. *J. Phys. Chem.* **1987**, *91*, 5149. (b) Yamabe, T.; Yoshizawa, K.; Matsuura, Y.; Tanaka, K. *Synth. Met.* **1995**, *75*, 55.

(33) Yamabe, T. *Conjugated Polymers and Related Materials*, Oxford University Press: Oxford, U.K., 1993; p 443.

(34) Tanaka, K.; Huang, Y.; Yamabe, T. *Phys. Rev. B* **1995**, *51*, 12715.

(35) Christides, C.; Neumann, D. A.; Prassides, K.; Copley, J. R. D.; Rush, J. J.; Rosseinsky, M. J.; Murphy, D. W.; Haddon, R. C. *Phys. Rev. B* **1992**, *46*, 12088.

(36) (a) Becke, A. D. *Phys. Rev. A* **1988**, *38*, 3098. (b) Becke, A. D. *J. Chem. Phys.* **1993**, *98*, 5648.

(37) Lee, C.; Yang, W.; Parr, R. G. *Phys. Rev. B* **1988**, *37*, 785.

(38) (a) Ditchfield, R.; Hehre, W. J.; Pople, J. A. *J. Chem. Phys.* **1971**, *54*, 724. (b) Hariharan, P. C.; Pople, J. A. *Theor. Chim. Acta* **1973**, *28*, 213.

(39) Frisch, M. J.; Trucks, G. W.; Schlegel, H. B.; Scuseria, G. E.; Robb, M. A.; Cheeseman, J. R.; Zakrzewski, V. G.; Montgomery, J. A.; Stratmann, R. E.; Burant, J. C.; Dapprich, S.; Millam, J. M.; Daniels, A. D.; Kudin, K. N.; Strain, M. C.; Farkas, O.; Tomasi, J.; Barone, V.; Cossi, M.; Cammi, R.; Mennucci, B.; Pomelli, C.; Adamo, C.; Clifford, S.; Ochterski, J.; Paterson, G. A.; Ayala, P. Y.; Cui, Q.; Morokuma, K.; Malick, D. K.; Rabuck, A. D.; Raghavachari, K.; Foresman, J. B.; Cioslowski, J.; Ortiz, J. V.; Stefanov, B. B.; Liu, G.; Liashenko, A.; Piskorz, P.; Komaromi, I.; Gomperts, R.; Martin, R. L.; Fox, D. J.; Keith, T.; Al-Laham, M. A.; Peng, C. Y.; Nanayakkara, A.; Gonzalez, C.; Challacombe, M.; Gill, P. M. W.; Johnson, B. G.; Chen, W.; Wong, M. W.; Andres, J. L.; Head-Gordon, M.; Replogle, E. S.; Pople, J. A.; *Gaussian 98*; Gaussian Inc.: Pittsburgh, PA, 1998.